



# Synthesis of nucleobase-neomycin conjugates and evaluation of their DNA binding, cytotoxicities, and antibacterial properties

Siwen Wang<sup>1</sup> · Mandeep Singh<sup>1</sup> · Mingheng Ling<sup>1</sup> · Danni Li<sup>1</sup> · Kregge M. Christison<sup>1</sup> · Joan Lin-Cereghino<sup>2</sup> · Geoff P. Lin-Cereghino<sup>2</sup> · Liang Xue<sup>1</sup>

Received: 28 November 2017 / Accepted: 16 March 2018  
© Springer Science+Business Media, LLC, part of Springer Nature 2018

## Abstract

Neomycin is known to preferentially bind to A-form nucleic acid structures including triplex DNA, DNA and RNA hybrid, and duplex RNA. Tethering a DNA intercalator moiety to the C5' position of the ring III of neomycin is a practical approach to develop potent binders targeting various nucleic acid secondary structures via a synergistic effect; however, the minimal stacking surface of the intercalating moiety required to exhibit the effect remains unclear. In the present work, we synthesized four nucleobase and neomycin conjugates via click chemistry. All four conjugates stabilized a DNA oligonucleotide triplex in the thermal denaturation experiments monitored by UV. The guanine-neomycin conjugate (**6b**) showed a better triplex stabilization effect than neomycin. All the conjugates, as well as neomycin, exhibited no thermal stabilization effect on a human telomeric DNA G-quadruplex. These results suggest that the synergistic effect of binding is vastly dependent on the surface area of the stacking moiety of the conjugates. In addition, tethering a nucleobase to the C5' position of neomycin enhanced the cytotoxicity of neomycin toward MCF-7 and HeLa cancer cells but decreased the antibacterial effect of neomycin against several Gram-negative and Gram-positive bacterial species.

**Keywords** Neomycin · DNA binding ligands · Cell viability · Antibacterial effect

## Abbreviations

Neo	neomycin	NMR	nuclear magnetic resonance
rRNA	ribosomal RNA	UHPLC	ultra-high-performance liquid chromatography
TAR	trans-activation response element	IR	infrared
AMEs	aminoglycoside-modifying enzymes	ESI	electrospray ionization
BQQ	benzo[f]quino[3,4-b]quinoxaline	HRMS	high-resolution mass spectrometry
DMSO	dimethyl sulfoxide	TOF	time of flight
MTT	3-(4,5-dimethylthiazol-2-yl)-2,5-diphenyltetrazolium bromide	FBS	fetal bovine serum
IC <sub>50</sub>	half maximal inhibitory concentration	DMEM	Dulbecco's modified eagle's medium
MIC	minimum inhibitory concentration	KB test	Kirby-Bauer test
		OD	optical density

These authors contributed equally: Siwen Wang, Mandeep Singh.

**Electronic supplementary material** The online version of this article (<https://doi.org/10.1007/s00044-018-2169-x>) contains supplementary material, which is available to authorized users.

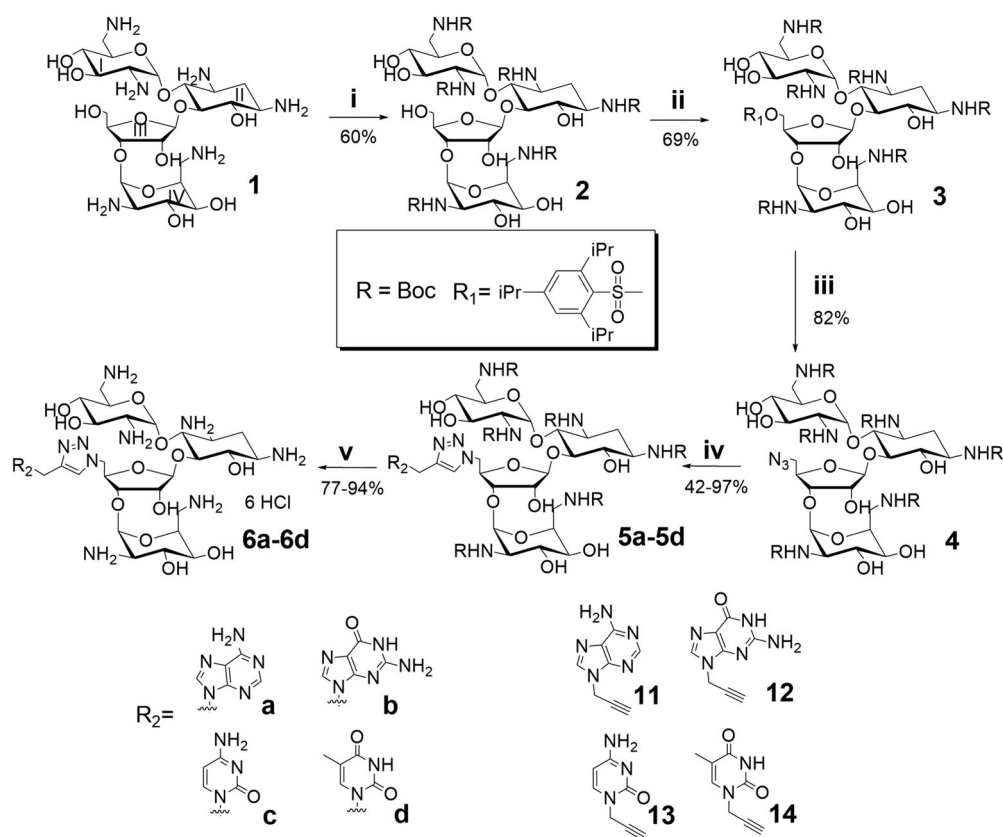
✉ Liang Xue  
lxue@pacific.edu

<sup>1</sup> Department of Chemistry, University of the Pacific, Stockton, CA 95211, USA

<sup>2</sup> Department of Biological Sciences, University of the Pacific, Stockton, CA 95211, USA

## Introduction

Neomycin, an aminoglycoside antibiotic, exerts its function by binding tightly to the A-site decoding region of bacterial ribosomal RNA (rRNA) and thus disrupting protein synthesis (Fourmy et al. 1998; Wong et al. 1998). Recent studies have revealed that neomycin also preferentially binds to A-form nucleic acid structures including triplex DNA, DNA and RNA hybrid, and duplex RNA (Arya et al.



**Scheme 1** Synthesis of nucleobase-neomycin conjugates (**6a–6d**). Reagents and conditions: i)  $(\text{Boc})_2\text{O}$ ,  $\text{DMF-H}_2\text{O}$ ,  $60^\circ\text{C}$ ; ii) 2,4,6-triisopropylbenzenesulfonyl chloride, pyridine, r.t.; iii)  $\text{NaN}_3$ ,  $\text{DMF}$ ,  $90^\circ\text{C}$ ; iv) **11–14**, sodium ascorbate,  $\text{CuSO}_4$ ,  $\text{DMF}$ , r.t.; v)  $4\text{MHCl}$  in Dioxane, r.t.

**2003c**). The binding specificity to nucleic acids results from its flexible oligosaccharide structure and multiple positive charges present under physiological conditions (Arya et al. **2003a**). Over the years, many neomycin based conjugates have been synthesized to target various nucleic acid structures. One of the major approaches for conjugation is to tether a moiety at the C5'' position of the ring III of neomycin (Scheme 1). Modification of this site has the least interference with the binding of neomycin to its target. An acridine-neomycin conjugate synthesized by Tor's group binds tightly to the HIV-1 Rev-Response Element (Kirk et al. **2000**). Several nucleobase-aminoglycoside conjugates exhibit increased binding affinities to the HIV-1 TAR and decreased affinities to the A-site of rRNA compared with the parent antibiotic (Blount and Tor **2006**). Arya and his coworkers have developed a series of neomycin based conjugates by coupling a DNA binding moiety such as intercalators with neomycin (Arya et al. **2003b**; Xue et al. **2002**). Most of the intercalator-neomycin conjugates show a better DNA triplex stabilization effect than both parent compounds (neomycin and intercalator). A perylene-neomycin conjugate developed by the same group shows a high binding affinity to human telomeric G-quadruplex DNA (Xue et al. **2011**). The enhanced DNA binding

affinities of these neomycin conjugates have been attributed to the synergistic effect (dual recognition mode), in which neomycin binds into a DNA groove while the other binding moiety stacks with DNA triplets or G-quartets.

Aminoglycosides are known for their inherent toxicity, usually nephrotoxicity (Oliveira et al. **2009**) or ototoxicity (Guthrie **2008**), due to their ability to sequester and generate redox active metal complexes that induce cell damage. However, in general, they are considered to be less cytotoxic toward tumor cells (e.g., MCF-7 cells, human breast adenocarcinoma) and nontumorigenic cells. Tethering a moiety to the C5'' of neomycin could result in a conjugate with unique cytotoxicity. Marchan and coworkers reported that a Ru(II) arene-neomycin complex displays moderate antiproliferative activity in MCF-7 cells and enhanced cytotoxicity in normal cells (Grau-Campistany et al. **2013**).

In recent years, the emergence of resistant bacteria, especially those containing aminoglycoside-modifying enzymes (AMEs) (Ramirez and Tolmasky **2010**), has become a global concern to public health. Modification of aminoglycosides is a useful approach to discover novel antibiotics (Green et al. **2010**; Houghton et al. **2010**). Ideally, the resulting aminoglycoside derivatives should still bind to their RNA receptor but cannot interact with AMEs.

The C5'' position has been used to design novel neomycin-based antibiotics to overcome the bacterial resistance to aminoglycosides that results from intensive clinical use. Chang and his coworkers developed a series of C5''-acylated neomycin derivatives and found two leads that exhibited prominent activity against both methicillin-resistant and vancomycin-resistant bacterial species (Zhang et al. 2009). Furthermore, bisubstrate derivatives consisting of adenosine and neamine (a truncated neomycin) using methylene groups as linkers were used as competitive inhibitors of aminoglycoside 3'-O-phosphotransferases (Liu et al. 2000).

In this report, we present the synthesis of four conjugates by coupling DNA nucleobases (adenine, guanine, thymine, and cytosine) to the C5'' position of neomycin via click chemistry. One goal of this research is to explore the size limitation of the aromatic surface in neomycin conjugates on their synergistic binding ability to DNA triplex and G-quadruplex. The previously reported conjugates contain a canonical DNA intercalator with a sizeable aromatic surface, so they are not suitable for this task. Native nucleobases are used here because they have a much smaller aromatic surface than DNA intercalators. In addition, the cytotoxicity against HeLa and MCF-7 cancer cells and antibacterial effect of these novel nucleobase-neomycin conjugates are of interest.

## Results and discussion

### Synthesis of nucleobase-neomycin conjugates

Nucleobases containing a propargyl group (**11–14** containing adenine, guanine, cytosine, and thymine, respectively) and C5''-azido neomycin (**4**) were prepared separately for the click reaction. The C5'' position of the ring III of neomycin (Scheme 1) was chosen for conjugation. The modification of this site has a minimal effect on the structure of neomycin and does not alter its charge distribution (amino groups). Tor's group has reported the direct attachment of three DNA bases (adenine, cytosine, and thymine) to neomycin for studying the selectivity toward two RNA targets (Blount and Tor 2006). Our conjugates are different from theirs by having a linker (1,2,3-triazole) between the nucleobase and neomycin. The presence of the linker may give additional flexibility to the nucleobase for an optimized intercalating position during the synergistic binding event.

The modification of neomycin was based on a previously published procedure (Kirk et al. 2000). All six amino groups of neomycin (**1**) were protected using di-tert-butyl dicarbonate to yield compound **2**. The 5'' primary hydroxyl group of **2** was converted into a good leaving group using

2,4,6-triisopropylbenzenesulfonyl chloride. Use of this bulky reagent enabled us to selectively react the 5'' primary hydroxyl group of neomycin. Replacement of 2,4,6-triisopropylbenzenesulfonylate in **3** with an azido group yielded compound **4**. Nucleobase derivatives **11–14** were synthesized based on previously published procedures (Edward Lindsell et al. 2000; Lu et al. 2007). The click reaction between propargyl nucleobases (**11–14**) and **4** afforded compounds **5a–5d** in the presence of catalytic amount of Cu (I), a catalyst that warrants the formation of 1,4-regioisomer of 1,2,3-triazole (Liu et al. 2011). Deprotection of the Boc groups from **5a–5d** using a dioxane solution saturated with HCl yielded the desired nucleobase-neomycin conjugates (**6a**: adenine-neomycin; **6b**: guanine-neomycin; **6c**: cytosine-neomycin; **6d**: thymine-neomycin) with a yield ranging from 77.0–93.5%. All the compounds were characterized by IR, <sup>1</sup>H NMR, and high-resolution ESI mass spectrometry. According to the <sup>1</sup>H NMR integration analysis, the purity of all final compounds (**6a–6d**) is no less than 95%, which is sufficient for the biochemical and biophysical studies conducted in the following session.

### The surface area of the aromatic moiety at the C5'' position of neomycin has a significant effect on the thermal stability of triplex DNA and G-quadruplex DNA

Thermal denaturation of triplex and G-quadruplex DNA in the presence of nucleobase-neomycin conjugates was carried out using UV spectroscopy. The triplex used was a short homooligomer dA<sub>22</sub>•2dT<sub>22</sub>. The G-quadruplex was formed from a human telomeric DNA fragment 5'-AGGG (TTAGGG)<sub>3</sub>T for this study. The UV wavelengths to monitor the melting of triplex and G-quadruplex DNA as a function of increasing temperature were 260 and 295 nm, respectively.

All the melting profiles of the triplex DNA are shown in Fig. 1a. In the absence of any ligand (control), the melting curve of dA<sub>22</sub>•2dT<sub>22</sub> shows a clear biphasic transition (hypochromic effect). The hyperchromicity observed at 8.7 °C represents a dissociation of triplex DNA into duplex DNA (dA<sub>22</sub>•dT<sub>22</sub>) and a single strand (dT<sub>22</sub>). This transition was readily observed at a temperature less than 10 °C using a recently published protocol (Xue et al. 2017). The dissociation of the remaining dA<sub>22</sub>•dT<sub>22</sub> into random coils is reflected by another hyperchromic effect observed at 54.1 °C. In order to compare the effect of various ligands on triplex stabilization, we chose a fixed concentration, 10 μM, to conduct the experiments. As shown in Table 1 and Fig. 1b, in the presence of neomycin, the dissociation temperature of triplex DNA (T<sub>m3→2</sub>) increases significantly to 39.3 °C, while the dissociation temperature of duplex DNA (T<sub>m2→1</sub>) is not affected. This observation is consistent with previous

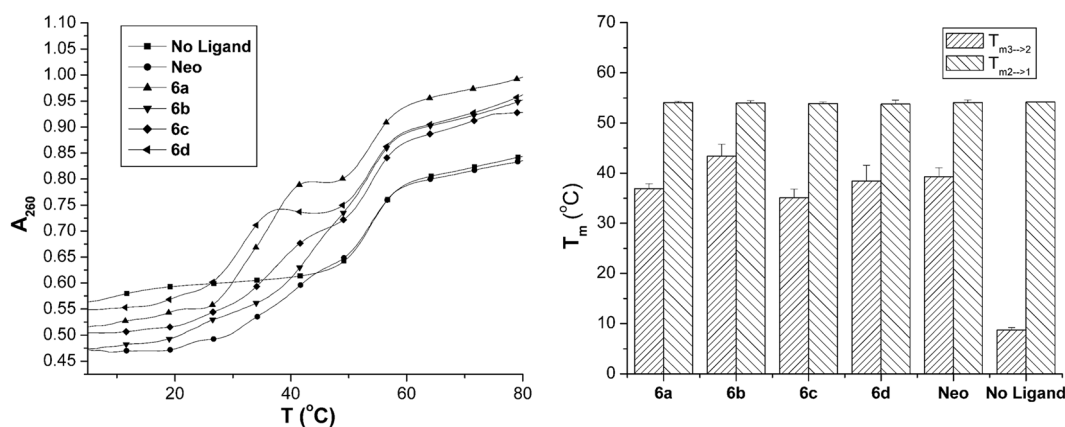


**Fig. 1** **a** UV melting profiles of a 22 mer T•A•T triplex (1  $\mu$ M) in the presence of neomycin (neo) and compound **6a–6d** (10  $\mu$ M). **b** Bar graphs showing the melting temperatures of triplex to duplex transition

( $T_{m3\rightarrow2}$ ) and duplex to random coil transition ( $T_{m2\rightarrow1}$ ). Buffer condition: 10 mM sodium cacodylate, 200 mM NaCl, 1 mM EDTA, pH 7.0

**Table 1** Temperatures of triplex to duplex transition ( $T_{m3\rightarrow2}$ ) and duplex to random coil transition ( $T_{m2\rightarrow1}$ ). The  $A_{22}\cdot 2T_{22}$  triplex was denaturated in the presence of neomycin (neo) and compound **6a–6d** (10  $\mu$ M)

Compound	$T_{m3\rightarrow2}$	$\Delta T_{m3\rightarrow2}$	$T_{m2\rightarrow1}$	$\Delta T_{m2\rightarrow1}$
<b>6a</b>	$36.9 \pm 1.0$	28.2	$54.1 \pm 0.2$	0
<b>6b</b>	$43.4 \pm 2.4$	34.7	$54.0 \pm 0.5$	-0.1
<b>6c</b>	$35.1 \pm 1.7$	26.4	$53.9 \pm 0.3$	-0.2
<b>6d</b>	$28.4 \pm 3.2$	19.7	$53.8 \pm 0.8$	-0.3
Neo	$39.3 \pm 1.8$	30.6	$54.1 \pm 0.5$	0
No Ligand	$8.7 \pm 0.5$	N/A	$54.1 \pm 0$	N/A

The  $\Delta T_m$  values were calculated based on the difference in the melting temperatures of the corresponding DNA in the presence and absence of a ligand

studies that neomycin stabilizes triplex DNA but not duplex DNA (Arya et al. 2003a). Neomycin snugly fits into the Watson-Hoogsteen groove of DNA triplex based on a computational study (Arya et al. 2003a). In the presence of a nucleobase-neomycin conjugate, a similar trend was observed. All four conjugates increase the  $T_{m3\rightarrow2}$  values but do not affect duplex melting temperatures as the  $\Delta T_{m2\rightarrow1}$  values are negligible (Table 1). Based on the  $\Delta T_{m3\rightarrow2}$  values, the order of triplex stabilization effect of these ligands is guanine-neomycin (**6b**) > neomycin (**neo**) > adenine-neomycin (**6a**) > cytosine-neomycin (**6c**) > thymine-neomycin (**6d**). Interestingly, the modification of the C5' position on the ring III of neomycin decreases neomycin's ability to stabilize DNA triplex because the  $T_{m3\rightarrow2}$  values in the presence of **6a**, **6c**, and **6d** are slightly less than that in the presence of neomycin. Adding a moiety at this position could sterically affect the binding of neomycin to the groove of triplex DNA. It is known that the binding pocket of neomycin is greatly affected by the surrounding structural geometry (Degtyareva et al. 2017). On the contrary,

we observed a 4.1 °C increment of  $T_{m3\rightarrow2}$  for **6b** as compared with that of neomycin, indicating a synergistic binding effect. In this case, the destabilization effect arising from the modification of the C5' position was rectified. The results reported here are consistent with the order for the stacking area ( $\text{\AA}^2$ ) of native nucleobases, which is guanine (G) > adenine (A) > cytosine (C) > thymine (T) (Guckian et al. 2000). The relatively larger stacking surface of guanine enables **6b** to bind to triplex DNA in a dual recognition mode. The guanine moiety sufficiently stacks with DNA triplets while the neomycin moiety binds into the groove of triplex DNA to form a stable complex. In addition, the exocyclic amino group of guanine may interact with T•A•T triplets and/or the backbone of DNA (Wellenzohn et al. 2001). However, **6b** cannot stabilize triplex DNA to the same extent as other conjugates with a much larger aromatic surface. Arya and coworkers developed a series of neomycin conjugates containing intercalators such as pyrene and BQQ (Arya et al. 2003b; Xue et al. 2002). They found that all of them exhibit significantly stronger triplex stabilization effect than neomycin. For instance, at a 4  $\mu$ M concentration, pyrene-neomycin showed an impressive 26 °C more increment of  $T_{m3\rightarrow2}$  for poly(dA)•2poly(dT) than neomycin. BQQ-neomycin bound to triplex DNA so tightly that only the direct dissociation of DNA triplex into random coils was observed. Their results indicate the importance of the aromatic surface for the dual recognition mode, which aligns well with our data. Further evidence for the role of the aromatic surface came from the thermal denaturation experiments of telomeric G-quadruplex DNA. Arya and coworkers reported a perylene diimide conjugated with two neomycin moieties that binds to G-quadruplex DNA with high affinity (Xue et al. 2011). The sizable aromatic surface of perylene facilitates the stacking of the molecule with G-quartets that are larger than DNA triplets. In our experiments, no increments in the  $T_m$  values of G-quadruplex

DNA were observed (Data not shown). Based on the CD spectrum (shown in the supporting information Fig. S9), the G-quadruplex DNA used in our study (Liu et al. 2017) could be a mixture of hybrid-type and basket-type conformations under the experimental conditions (50 mM K<sup>+</sup>) (Ambrus et al. 2006). G-quartets have a much larger surface than DNA triplets so relatively small nucleobases could not sufficiently stack with them. Furthermore, neomycin does not thermally stabilize G-quadruplex DNA. These data indicate that a synergistic binding requires at least one moiety with a strong binding affinity to the DNA target. The first binding moiety could serve as an anchor to facilitate the binding of the second moiety. The size of the aromatic surface of intercalator-neomycin conjugates affects the binding specificity. Taken together, we conclude that the size of guanine could be a minimum requirement for developing intercalator-neomycin conjugates to target triplex DNA in a synergistic manner. Intercalator-neomycin conjugates that bind to G-quadruplex DNA require a much larger intercalator moiety to stack with G-quartets efficiently.

### Nucleobase-neomycin conjugates are more cytotoxic than neomycin

The cytotoxicity of nucleobase-neomycin conjugates against two cancer cell lines (MCF-7 and HeLa) was measured using the MTT assay. In this assay, the absorbance of a reduction product (formazan) from a tetrazolium salt (MTT) is determined spectroscopically. Only live cells can release active reductases that catalyze the reduction reaction; therefore, the absorbance of formazan is proportional to the number of live cells in culture. Because neomycin was reported to have minimal cytotoxicity toward MCF-7 cells (IC<sub>50</sub> > 250 μM) (Grau-Campistany et al. 2013), we used a higher concentration (500 μM) for the initial test. The results from the MTT assay are shown in Fig. 2. Neomycin shows little cytotoxicity toward both cell lines as expected. The viability values of MCF-7 and HeLa cells in the presence of 500 μM neomycin are (94.6 ± 12.5) and (96.4 ± 1.5)%, respectively. In general, all nucleobase-neomycin derivatives are more cytotoxic toward both cancer cell lines than neomycin in a statistically significant manner (*p* < 0.05). All nucleobase-neomycin derivatives except for **6d** are more cytotoxic toward HeLa cells than MCF-7 cells. The orders of increasing cytotoxicity are **neo** < **6a** < **6d** < **6c** < **6b** for HeLa cells and **neo** < **6d** < **6a** < **6c** < **6b** for MCF-7 cells. In both cases, **6b** (guanine-neomycin) is the most cytotoxic, and it is more effective in reducing the HeLa cell viability. The HeLa cell viability (%) in the presence of 500 μM **6b** is (15.4 ± 0.8)%, at least 2-fold less than those values of the other three conjugates. By contrast, the MCF-7 cell viability (%) in the presence of 500 μM **6b** is only (47.6 ± 6.7)%. The cell

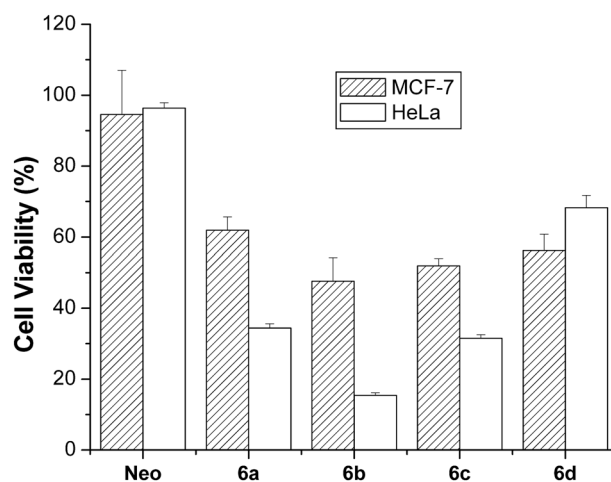


**Fig. 2** Cytotoxic effect of neomycin and compounds **6a–6d** (500 μM) in the MCF-7 and HeLa cancer cell lines. Cell viability was determined by the MTT assay

viability values of the four conjugates for MCF-7 cells range from 47.6 to 61.9%. The difference in values is much smaller than that for HeLa cells (15.4–68.3%). These data indicate that all nucleobase-neomycin conjugates have differential cytotoxicity toward MCF-7 and HeLa cancer cells, which could result from the cell uptake efficiency. The conjugate **6b** with the largest stacking moiety gave the most prominent effect on reduction in cell viability, but the correlation between the stacking moiety and cytotoxicity could not be drawn. The observed cytotoxicity could result from binding of these conjugates to other cellular targets such as RNA (Degtyareva et al. 2017; Kirk et al. 2000). No further concentration-dependent studies were carried out as the IC<sub>50</sub> values for these conjugates would be higher than 250 μM (considered to be inactive) (Grau-Campistany et al. 2013). Conjugation of a nucleobase moiety to the C5' of neomycin leads to the enhanced cytotoxicity toward two cancer cell lines used here. The increase in the cytotoxicity of neomycin by tethering a Ru (II) moiety at the same position has been previously reported (Grau-Campistany et al. 2013). However, the factors attributed to the enhanced cytotoxicity reported in the paper were more complicated because the Ru (II) moiety itself could induce cell damage via redox reactions. Because nucleobases are not cytotoxic, the increased cytotoxicity observed by us could merely result from the structural change at the C5' position of neomycin. Hence, tethering a moiety to the C5' of neomycin could be a useful approach to design aminoglycoside based cytotoxic reagents.

### Nucleobase-neomycin conjugates inhibit bacterial growth less efficiently than neomycin

We investigated the antibacterial effect of nucleobase-neomycin conjugates on aminoglycoside resistant and non-resistant bacterial species.

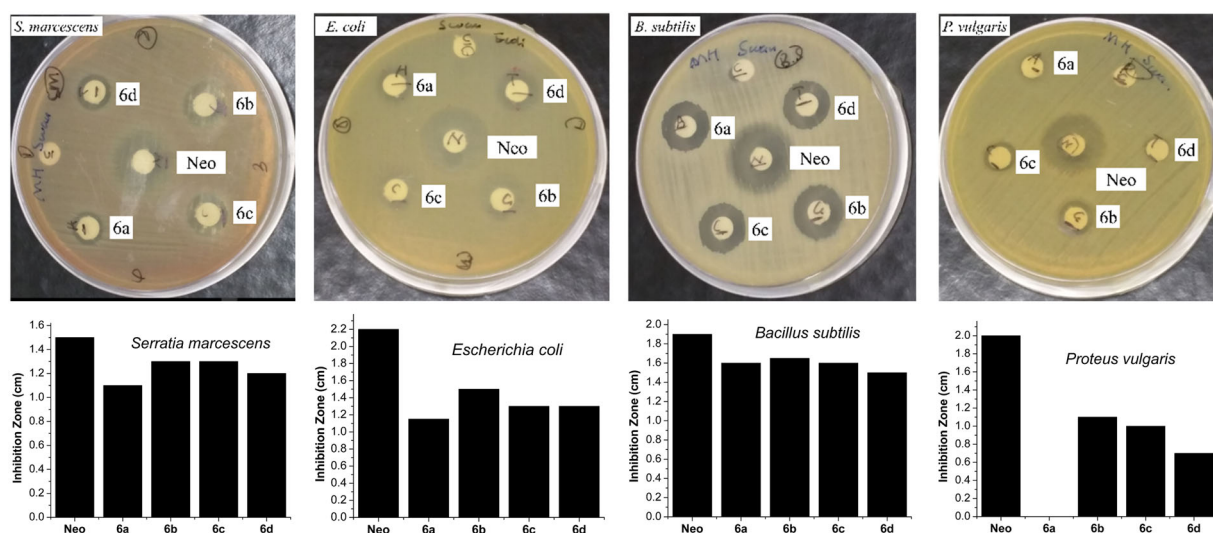


**Fig. 3 a** Petri dish images (Kirby–Bauer Test) showing the zone of inhibition by compound **6a–6d** (50 nmol) against various bacterial species (*S. marcescens* (Gram negative), *E. coli* (Gram negative), *B.*

*subtilis* (Gram positive), and *P. vulgaris* (Gram negative)). Neomycin (50 nmol) was used as a control. **b** Diameter values of the zone of inhibition for each compound

All nucleobase-neomycin conjugates (50 nmol) were first assayed (Fig. 3a) against four antibiotic-susceptible species including *Serratia marcescens* (*S. marcescens*, Gram negative), *Escherichia coli* (*E. coli*, Gram negative), *Bacillus subtilis* (*B. subtilis*, Gram positive), and *Proteus vulgaris* (*P. vulgaris*, Gram negative) using the Kirby–Bauer (agar disk-diffusion) test (Balouiri et al. 2016). Neomycin with the same amount was used as a control. The inhibition of bacterial growth is positively related to the inhibition-zone size on agar, in which no bacterial growth occurs. The diameters of inhibition zones were directly measured using a ruler (Fig. 3b). The values (cm) of the inhibition zone of neomycin are 1.5 for *S. marcescens*, 2.2 for *E. coli*, 1.9 for *B. subtilis*, and 2.0 for *P. vulgaris*. We calculated the median values of inhibition zones of four conjugates for each bacterial species. The values (cm) are 1.2 for *S. marcescens*, 1.3 *E. coli*, 1.6 for *B. subtilis*, and 0.7 for *P. vulgaris*. By subtracting these median values from the values of the inhibition zone of neomycin for each bacterial species (0.3 cm for *S. marcescens*, 0.9 cm for *E. coli*, 0.3 cm for *B. subtilis*, and 1.3 cm for *P. vulgaris*), we elucidated the effect of conjugation on the antibacterial activity of neomycin. Neomycin gives the best inhibitory effect against all four bacterial species compared with nucleobase–neomycin conjugates. Conjugation of nucleobases reduces the antibacterial activity of neomycin. Modification of the C5'-position could decrease the binding of neomycin to its target rRNA. The reduction effect is bacterial species dependent. Conjugation of nucleobases to neomycin has less effect on reduction in the antibacterial activity of neomycin against *S. marcescens* and *B. subtilis*. *B. subtilis* is a Gram-positive bacterium so the decreased reduction effect on this species could result from

a different inhibitory mechanism or a different mechanism of cellular penetration through the outer membranes between Gram-negative and Gram-positive bacteria. Conjugation of nucleobases to neomycin significantly reduces the antibacterial activity of neomycin against *E. coli* and *P. vulgaris*. We observed the greatest reduction effect for the latter. Amongst all the nucleobase-neomycin derivatives, **6b** is more active against all four bacterial species, and the compound **6a** is the least active compound against the three Gram-negative bacterial species. It is noteworthy that adenine-neomycin (**6a**) does not show a detectable inhibition zone for *P. vulgaris* at the concentration we used.

The minimum inhibitory concentrations (MICs) of nucleobase-neomycin conjugates against four bacterial species were further determined on 96-well microtiter plates. The OD<sub>600</sub> value of the well in the absence of bacteria was used as a control, representing a complete inhibition effect of bacterial growth. The results are shown in Fig. 4 and Table S1 of the supporting information. The MIC values of neomycin toward *E. coli* and *B. subtilis* are comparable to previously reported values (Fridman et al. 2003). The order of bacterial species regarding decreasing inhibitory effect by the compounds is *B. subtilis* > *E. coli* > *S. marcescens* > *P. vulgaris*. All compounds inhibit the growth of the Gram-positive bacterium, *B. subtilis*, more efficiently than that of any Gram-negative bacteria. This data is consistent with the Kirby–Bauer test mentioned above. While none of the conjugates exhibits a better inhibitory effect than the parent neomycin for all the species, the compound **6b** inhibits the bacterial growth more efficiently than the other three conjugates. The reduction in the inhibition of bacterial growth is more significant for Gram-negative than Gram-positive bacteria. For instance,

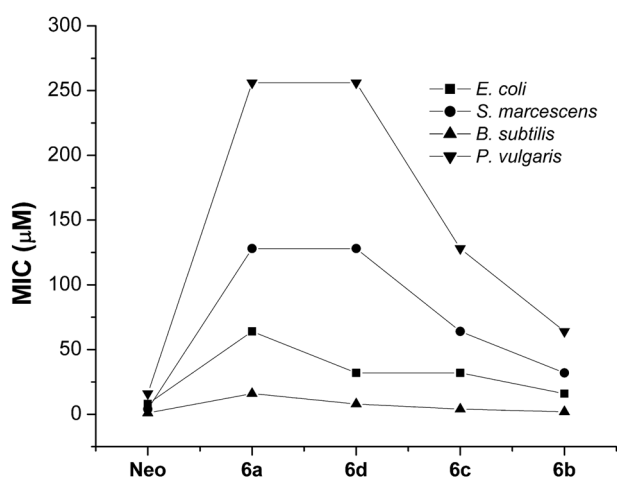


**Fig. 4** Minimal inhibition concentrations (MIC) of neomycin and compound **6a–6d** against various bacterial species (*S. marcescens* (Gram negative), *E. coli* (Gram negative), *B. subtilis* (Gram positive), and *P. vulgaris* (Gram negative))

the MIC value of **6b** against *B. subtilis* is 2 nmol/mL, only two-fold more than that of neomycin. The MIC value of **6b** against *S. marcescens* is 32 nmol/mL, eight-fold more than that of neomycin. With limited data, no relationships between the stacking surface of nucleobases and antibacterial effect could be ascertained at this point.

The inhibition of bacterial growth by these conjugates was also investigated using an *E. coli* strain that was transfected with an aminoglycoside 3'-O-phosphotransferase (APHs) Ia gene. This strain is known to have a resistance profile including kanamycin, neomycin, and a few other aminoglycosides (Vakulenko and Mobashery 2003). The resistance to aminoglycosides results from the transfer of a phosphate group to the 3' or 5'' hydroxyl group of the aminoglycoside molecule and thus affecting its binding to the target rRNA (Vakulenko and Mobashery 2003). Nucleobase-neomycin conjugates have modified structures that could block the binding to APHs and thus inhibit its function for phosphorylation. We were only able to obtain two MICs values for neomycin and **6b**, respectively, even when the concentration was used at as high as 512 μM. The MIC value (64 μM) of neomycin for this strain is 8-fold larger than that for un-transfected *E. coli*, indicating the presence of drug resistance. The effect of resistance to kanamycin is much stronger as no MIC value was observed (Table S1 of the supporting information). The compound **6b** displays a MIC value of 512 μM toward the transfected strain, which is 32-fold more than that (16 μM) for the un-transfected species. These results suggest that none of the nucleobase-neomycin conjugates can overcome the bacterial resistance as their MIC values are all worse than that of neomycin for this species. Tethering a nucleobase moiety to the C5'' position of neomycin does not alter the binding of aminoglycoside 3'-O-phosphotransferase to

these conjugates. It is reasonable that the nucleobase moiety may not be large enough to interfere with the binding.

## Conclusion

We have completed the synthesis of four novel nucleobase-neomycin conjugates. The results from the thermal denaturation of triplex DNA, together with the reports by others, suggest that the stacking size of guanine could be the minimal limit for neomycin conjugates in the same category to exert the synergistic binding effect. Judging from the melting data, we conclude that the synergistic effect requires at least one moiety to have a strong binding affinity to the target. Modification of the C5'' position of neomycin is an effective approach to enhance the cytotoxicity of an aminoglycoside (neomycin) against two cancer cell lines used in this research. Based on the antibacterial profile, tethering a nucleobase to the C5'' position of neomycin could affect the binding of neomycin to its rRNA target but this modification does not block the function of aminoglycoside 3'-O-phosphotransferase. Our results presented here provide useful information for developing aminoglycoside-based compounds with better binding affinities, enhanced antibacterial activities, and altered toxicities.

## Experimental section

### Materials and methods

Chemicals for synthesis were purchased from Fisher Scientific (Pittsburgh, PA) and used without further purification. Reactions were carried out under Argon using dry solvent unless otherwise noted. IR spectra were collected on a Shimadzu (Pleasanton, CA) IR Prestige-21 FT-IR spectrophotometer. <sup>1</sup>H NMR spectra were collected on a JEOL (Peabody, MA) ECA 600 MHz FT-NMR spectrometer. HRMS (ESI) spectra were collected on an Agilent (Santa Clara, CA) 1290 UHPLC connected to an Agilent 6230 TOF mass spectrometer through an electrospray ionization source. UV spectra were collected on a Varian Cary 100 Bio UV-Vis spectrophotometer equipped with a thermoelectrically controlled 6 × 6 cell holder (Walnut Creek, CA). The MTT read-outs were measured by a TriStar LB 941 multimode microplate reader. Dulbecco's modified eagle's medium (DMEM) was purchased from Sigma (St. Louis, MO). Advanced MEM, glutamax, penicillin, and streptomycin were purchased from Invitrogen (Carlsbad, CA). Fetal bovine serum (FBS) was purchased from Tissue Culture Biologicals (Seal Beach, CA).

### Synthesis of 5a

Adenine-9-prop-2ynyl (**11**) (12.5 mg, 0.072 mmol) was added to an anhydrous DMF solution (6 mL) of sodium ascorbate (13.7 mg, 0.069 mmol), copper (II) sulfate (2.0 mg, 0.008 mmol), and compound **4** (71.0 mg, 0.058 mmol). The reaction mixture was stirred at room temperature overnight. The completion of the reaction was monitored by TLC (silica gel 60 F<sub>254</sub>, EMD Millipore) under UV ( $R_f=0.23$ , CH<sub>3</sub>OH:CH<sub>2</sub>Cl<sub>2</sub> 0.8:9.2 v/v). The reaction mixture was concentrated under vacuum. Flash chromatography of the residue (silica gel, CH<sub>3</sub>OH:CH<sub>2</sub>Cl<sub>2</sub> 1:9 v/v) yielded compound **5a** (67.5 mg, 82.0%) as a pale white solid. IR (KBr) (cm<sup>-1</sup>) 3343, 2976, 2938, 1644, 1649, 1631, 1367, 1248, 1165, 1043. <sup>1</sup>H NMR (CD<sub>3</sub>OD, 600 MHz)  $\delta$  8.32 (s, 1H), 8.22–8.29 (m, 2H), 6.47–6.83 (m, 2H), 5.58–5.70 (m, 1H), 5.33–5.44 (bs, 1H), 5.01–5.11 (m, 1H), 4.97 (s, 1H), 4.78–4.86 (m, 1H), 4.66–4.76 (m, 1H), 4.07–4.41 (m, 3H), 3.98 (t, 1H,  $J=5.8$  Hz), 3.90 (s, 1H), 3.66–3.83 (m, 3H), 3.50–3.65 (m, 2H), 3.41–3.49 (m, 2H), 2.98–3.08 (m, 1H), 1.90–2.01 (m, 1H), 1.15–1.56 (m, 54H). HRMS (ESI) calcd. for C<sub>61</sub>H<sub>100</sub>N<sub>14</sub>O<sub>24</sub> [M + H]<sup>+</sup> 1413.7113, found 1413.7090.

### Synthesis of 5b

Guanine-9-prop-2ynyl (**11**) (14.0 mg, 0.074 mmol) was added to an anhydrous DMF solution (6 mL) of sodium ascorbate (15.0 mg, 0.075 mmol), copper (II) sulfate (3.0 mg, 0.012 mmol), and compound **4** (46.0 mg, 0.037 mmol). The reaction mixture was stirred at room temperature overnight. The completion of the reaction was monitored by TLC (silica gel 60 F<sub>254</sub>, EMD Millipore) under UV ( $R_f=0.275$ , CH<sub>3</sub>OH:CH<sub>2</sub>Cl<sub>2</sub>:NH<sub>4</sub>OH 1.25:8.75:0.1 v/v/v). The reaction mixture was concentrated under vacuum. Flash chromatography of the residue (silica gel, CH<sub>3</sub>OH:CH<sub>2</sub>Cl<sub>2</sub>:NH<sub>4</sub>OH 1.25:8.75:0.1 v/v/v) yielded compound **5b** (25.0 mg, 47.3%) as a pale white solid. IR (KBr) (cm<sup>-1</sup>) 3408, 1689, 1633, 1516, 13676, 1251, 1167, 1043, 856. <sup>1</sup>H NMR (CD<sub>3</sub>OD, 600 MHz)  $\delta$  8.36 (s, 1H), 7.83 (s, 1H), 6.62–6.84 (m, 1H), 5.56 (d,  $J=14.4$  Hz, 1H), 5.36 (s, 1H), 5.28 (d,  $J=15.6$  Hz, 1H), 5.01 (s, 1H), 4.96 (s, 1H), 4.61–4.73 (m, 1H), 3.90–4.15 (m, 4H), 3.87 (s, 1H), 3.68–3.79 (m, 2H), 3.38–3.59 (m, 7H), 3.28–3.37 (m, 1H), 3.04 (br s, 1H), 1.84–1.96 (m, 1H), 1.25–1.49 (m, 54H). HRMS (ESI) calcd. for C<sub>61</sub>H<sub>100</sub>N<sub>14</sub>O<sub>25</sub> [M + H]<sup>+</sup> 1429.7062, found 1429.7042.

### Synthesis of 5c

Cytosine-1-prop-2ynyl (**13**) (24.0 mg, 0.161 mmol) was added to an anhydrous DMF solution (6 mL) of sodium ascorbate (14.6 mg, 0.0738 mmol), copper (II) sulfate

(2.0 mg, 0.008 mmol), and compound **4** (64.0 mg, 0.054 mmol). The reaction mixture was stirred at room temperature overnight. The completion of the reaction was monitored by TLC (silica gel 60 F<sub>254</sub>, EMD Millipore) under UV ( $R_f=0.435$ , CH<sub>3</sub>OH:CH<sub>2</sub>Cl<sub>2</sub>:NH<sub>4</sub>OH 1.5:8.5:0.05 v/v/v). The reaction mixture was concentrated under vacuum. Flash chromatography of the residue (silica gel, CH<sub>3</sub>OH:CH<sub>2</sub>Cl<sub>2</sub> 1.25:8.75 v/v) yielded compound **5c** (30.0 mg, 42.0%) as a pale white solid. IR (KBr) (cm<sup>-1</sup>) 3369, 2978, 2932, 1701, 1647, 1524, 1394, 1367, 1280, 1251, 1169, 1043, 865. <sup>1</sup>H NMR (CD<sub>3</sub>OD, 600 MHz)  $\delta$  8.07 (s, 1H), 7.73 (d,  $J=7.26$  Hz, 1H), 5.85 (d,  $J=7.26$  Hz, 1H), 5.47 (s, 1H), 5.41 (s, 1H), 5.00–5.13 (m, 3H), 4.92 (d,  $J=1.56$  Hz, 1H), 4.66 (dd,  $J=13.02$  Hz, 4.38 Hz, 1H), 4.58 (s, 1H), 4.07–4.36 (m, 3H), 3.95 (m, 1H), 3.88 (s, 1H), 3.69–3.79 (m, 2H), 3.57–3.67 (m, 1H), 3.39–3.55 (m, 4H), 3.31–3.38 (m, 2H), 3.09 (m, 1H), 1.86–1.97 (m, 1H), 1.25–1.49 (m, 54H). HRMS (ESI) calcd. for C<sub>61</sub>H<sub>100</sub>N<sub>14</sub>O<sub>25</sub> [M + H]<sup>+</sup> 1389.7001, found 1389.6990.

### Synthesis of 5d

Thymine-1-prop-2ynyl (**14**) (13.7 mg, 0.0836 mmol) was added to an anhydrous DMF solution (6 mL) of sodium ascorbate (15.8 mg, 0.079 mmol), copper (II) sulfate (2.0 mg, 0.008 mmol), and compound **4** (55.0 mg, 0.0442 mmol). The reaction mixture was stirred at room temperature overnight. The completion of the reaction was monitored by TLC (silica gel 60 F<sub>254</sub>, EMD Millipore) under UV ( $R_f=0.2125$ , CH<sub>3</sub>OH:CH<sub>2</sub>Cl<sub>2</sub> 0.75:9.25 v/v). The reaction mixture was concentrated under vacuum. Flash chromatography of the residue (silica gel, CH<sub>3</sub>OH:CH<sub>2</sub>Cl<sub>2</sub> 0.75:9.25 v/v) yielded compound **5d** (60.0 mg, 96.7%) as a pale white solid. IR (KBr) (cm<sup>-1</sup>) 3371, 2978, 2934, 1690, 1514, 1458, 1392, 1367, 1267, 1250, 1167, 1043, 862, 781. <sup>1</sup>H NMR (CD<sub>3</sub>OD, 600 MHz)  $\delta$  8.10 (s, 1H), 7.56 (s, 1H), 6.55–6.67 (m, 1H), 6.37–6.53 (m, 1H), 5.47 (s, 1H), 5.41 (s, 1H), 4.89–5.14 (m, 3H), 4.54–4.68 (m, 1H), 4.04–4.47 (m, 3H), 3.95 (t,  $J=6.6$  Hz, 1H), 3.70–3.80 (m, 2H), 3.60–3.69 (m, 1H), 3.36–3.59 (m, 3H), 3.08 (t,  $J=8.4$  Hz, 1H), 1.87–1.95 (m, 1H), 1.85 (d,  $J=1.3$  Hz, 3H), 1.25–1.48 (m, 54H). HRMS (ESI) calcd. for C<sub>61</sub>H<sub>101</sub>N<sub>11</sub>O<sub>26</sub> [M + H]<sup>+</sup> 1404.6997, found 1404.6971.

### General procedure for the synthesis of 6a–6d

Hydrochloric acid in dioxane (4 M, 1 mL) and ethanedithiol (3  $\mu$ L) were added into a dioxane solution (1 mL) of compound **5a** (17.0 mg), **5b** (24.0 mg), **5c** (12.0 mg), or **5d** (24.0 mg) in a 15-mL conical vial. The reaction mixture was swirled for 5 min and became turbid. The deprotected product was further precipitated by adding ether and hexane (1 mL each). The solid was collected by centrifugation

(3000 r.p.m.), decanted, washed with ether (3 × 1 mL) and hexane (3 × 1 mL), and dried overnight under vacuum. The residue was re-dissolved in milli-Q water and lyophilized to give a pale-white fluffy solid.

#### Compound 6a

Yield: 11.6 mg, 93.5%. IR (KBr) (cm<sup>-1</sup>) 3396, 3058, 2948, 1685, 1601, 1491, 1144, 1044, 1018, 769, 638. <sup>1</sup>H NMR (D<sub>2</sub>O, 600 MHz) δ 8.32 (s, 1H), 8.30 (s, 1H), 8.17 (s, 1H), 5.94 (d, *J* = 4.2 Hz, 1H), 5.56 (s, 2H), 5.31 (d, *J* = 3.6 Hz, 1H), 5.21 (d, *J* = 1.8 Hz, 1H), 4.76 (dd, *J* = 15.0 Hz, 5.0 Hz, 1H), 4.68 (m, 1H), 4.45 (m, 2H), 4.23 (m, 1H), 4.12 (t, *J* = 6.0 Hz, 1H), 4.05 (t, *J* = 9.6 Hz, 1H), 3.82–3.93 (m, 4H), 3.72 (s, 1H), 3.62 (t, *J* = 9.6 Hz, 1H), 3.21–3.51 (m, 9H), 2.38 (m, 1H), 1.82 (m, 1H). HRMS (ESI) calcd. for C<sub>31</sub>H<sub>53</sub>N<sub>14</sub>O<sub>12</sub><sup>+</sup> [M + H]<sup>+</sup> 813.3962, found 813.3945.

#### Compound 6b

Yield: 14.7 mg, 84.0%. IR (KBr) (cm<sup>-1</sup>) 3383, 2922, 1701, 1637, 1604, 1500, 1490, 1369, 1143, 1047, 1024, 781, 605. <sup>1</sup>H NMR (D<sub>2</sub>O, 600 MHz) δ 8.16 (s, 1H), 8.05 (s, 1H), 5.52 (d, *J* = 4.2 Hz, 1H), 5.34 (s, 2H), 5.23 (d, *J* = 4.2 Hz, 1H), 5.19 (d, *J* = 1.2 Hz, 1H), 4.71–4.75 (m, 1H), 4.65 (s, 1H), 4.43 (q, *J* = 4.2 Hz, 1H), 4.38 (t, *J* = 4.8 Hz, 1H), 4.20 (t, *J* = 4.8 Hz, 1H), 4.09 (t, *J* = 3 Hz, 1H), 3.74–3.90 (m, 4H), 3.70 (s, 1H), 3.17–3.51 (m, 11H), 2.35 (dt, *J* = 8.4 Hz, 4.2 Hz, 1H), 1.75–1.86 (m, 1H). HRMS (ESI) calcd. for C<sub>31</sub>H<sub>53</sub>N<sub>14</sub>O<sub>13</sub><sup>+</sup> [M + H]<sup>+</sup> 829.3911, found 829.3909.

#### Compound 6c

Yield: 6.7 mg, 77.0%. IR (KBr) (cm<sup>-1</sup>) 3392, 1676, 1497, 1144, 1053, 1018, 797. <sup>1</sup>H NMR (D<sub>2</sub>O, 600 MHz) δ 8.08 (s, 1H), 7.83 (d, *J* = 7.8 Hz, 1H), 6.04 (d, *J* = 7.2 Hz, 1H), 5.93 (d, *J* = 3.0 Hz, 1H), 5.30 (d, *J* = 2.4 Hz, 1H), 5.22 (s, 1H), 5.02 (s, 2H), 4.55–4.84 (m, 2H), 4.45 (s, 2H), 4.24 (t, *J* = 3.6 Hz, 1H), 4.12 (s, 1H), 4.05 (t, *J* = 9.6 Hz, 1H), 3.77–3.99 (m, 4H), 3.73 (s, 1H), 3.60 (t, *J* = 10.2 Hz, 1H), 3.19–3.55 (m, 9H), 2.38 (m, 1H), 1.83 (q, *J* = 12.0 Hz, 1H). HRMS (ESI) calcd. for C<sub>30</sub>H<sub>53</sub>N<sub>14</sub>O<sub>12</sub><sup>+</sup> [M + H]<sup>+</sup> 789.3850, found 789.3859.

#### Compound 6d

Yield: 14.7 mg, 84.0%. IR (KBr) (cm<sup>-1</sup>) 3387, 2918, 1701, 1601, 1244, 1220, 1143, 1049, 1026, 773. <sup>1</sup>H NMR (D<sub>2</sub>O, 600 MHz) δ 8.03 (s, 1H), 7.51 (d, *J* = 1.2 Hz, 1H), 5.82 (d, *J* = 3.6 Hz, 1H), 5.28 (d, *J* = 3.6 Hz, 1H), 5.21 (d, *J* = 1.2 Hz, 1H), 4.94 (d, *J* = 2.4 Hz, 2H), 4.75 (dd, *J* = 15.0 Hz, 3.0 Hz, 1H), 4.56–4.72 (m, 1H), 4.39–4.48 (m, 2H), 4.20–4.25 (m, 1H), 4.11 (t, *J* = 3.0 Hz, 1H), 3.84–3.96

(m, 3H), 3.74–3.83 (m, 2H), 3.69–3.73 (m, 1H), 3.54 (t, *J* = 10.2 Hz, 1H), 3.47–3.51 (m, 1H), 3.20–3.46 (m, 8H), 2.32 (m, 1H), 1.70–1.82 (m, 4H). HRMS (ESI) calcd. for C<sub>31</sub>H<sub>54</sub>N<sub>11</sub>O<sub>14</sub><sup>+</sup> [M + H]<sup>+</sup> 804.3846, found 804.3850.

#### Measurements of high-resolution mass spectra

Samples were introduced by flow injection analysis (FIA) in positive-ion mode. The mobile phase was 90% H<sub>2</sub>O and 10% MeOH with 0.1% formic acid. The nebulizer pressure was 50 psi with 12 L/min of nitrogen (drying gas) at 325 °C for desolvation. The capillary voltage was set at 3500 V, the fragmentor voltage was set at 150 V, the skimmer voltage was set at 65 V, and the octopole voltage was set at 750 V. Spectra were collected from 300–1500 Da at a rate of 2 spectra/sec with 4962 transients/spectrum.

#### Preparation of triplex DNA for thermal denaturation

The oligonucleotides dA<sub>22</sub> (1 μM) and dT<sub>22</sub> (2 μM) were mixed with a solution (1 mL, pH 7.0) of sodium cacodylate (10 mM), EDTA (1 mM), and sodium chloride (200 mM) in the absence or presence of a ligand (10 μM). The mixtures were heated at 90 °C for 5 min, slowly cooled at 25 °C, and incubated at 4 °C overnight before use.

#### Preparation of G-quadruplex DNA for thermal denaturation

The G-quadruplex sequence 5'-AGG(TTAGGG)<sub>3</sub>T (1 μM) was mixed with a solution (1 mL, pH 7.0) of lithium cacodylate (10 mM), EDTA (1 mM), and potassium chloride (50 mM) in the absence or presence of a ligand (10 μM). The mixtures were heated at 90 °C for 5 min, slowly cooled at 25 °C, and incubated at 4 °C overnight before use.

#### Thermal denaturation of triplex DNA or G-quadruplex DNA

UV melting spectra were recorded at 260 nm for triplex DNA and 295 nm for G-quadruplex DNA as a function of increasing temperature (4–80 °C, heating rate: 0.5 °C/min). The melting temperatures (*T*<sub>m</sub>) were determined using the first derivative method.

#### The MTT assay

All the experiments were carried out in triplicate. MCF-7 (human breast adenocarcinoma) and HeLa cells were maintained in advanced DMEM medium supplemented with 5% fetal bovine serum (FBS), L-glutamine and antimycotic (antibiotic) at 37 °C in a humid atmosphere containing 5% CO<sub>2</sub>. Neomycin and nucleobase-neomycin

conjugates (**6a–6b**) were pre-dissolved in sterilized water. The cells (3000 cells/well, 200  $\mu\text{L}$ ) were seeded in a 96-well microtiter plate and incubated for 24 h. The supernatant in each well was removed followed by adding neomycin or conjugates in FBS free media (200  $\mu\text{L}$ ) to reach a final concentration of 500  $\mu\text{M}$ . After incubation at 37  $^{\circ}\text{C}$  for 72 h, an MTT solution (20  $\mu\text{L}$ , 0.5 mg/mL) was added to each well and incubated for 4 h. The formazan product was dissolved in 150  $\mu\text{L}$  of DMSO, and the absorbance of each well was measured at 590 nm using a plate reader. Untreated cells and media without cells were used as controls.

To calculate the viability (%), the following equation was used.

$$\text{Viability (\%)} = \frac{(A_{\text{treated}}) - (A_{\text{media}})}{(A_{\text{untreated}}) - (A_{\text{media}})} \times 100\%$$

$A_{\text{treated}}$ : The absorbance of the solution containing treated cells  $A_{\text{media}}$ : The absorbance of the media  $A_{\text{untreated}}$ : The absorbance of the solution containing untreated cells

### Statistical analysis

Minitab software was used to determine the statistical significance. Two-sample student's *t*-test was performed to show statistically significant ( $p < 0.05$ ) and insignificant ( $p > 0.05$ ) data.

### Kirby–Bauer test protocol (Disk diffusion zone determination)

Neomycin or conjugate (50 nmol) impregnated paper discs were placed onto the surface of Müller Hinton agar plates (70191 Fluka) that were pre-seeded with bacteria (*Bacillus subtilis*, *Escherichia coli*, *Proteus vulgaris*, and *Serratia marcescens*) and incubated aerobically at 37  $^{\circ}\text{C}$  for 24 h. The diameters of inhibition zones were measured using a ruler to the nearest 1 mm.

### Determination of minimum inhibition concentrations (MICs)

Bacterial species were grown overnight in the Müller Hinton broth at 37  $^{\circ}\text{C}$ . A dilution of the overnight culture was made in broth to an approximate concentration of  $10^6$  cfu/mL. A Müller Hinton broth (100  $\mu\text{L}$ ) solution containing the desired antibacterial reagent (neomycin or compound **6a–6d**) was inoculated with a freshly diluted bacterial suspension (5  $\mu\text{L}$ ) in a 96-well plate and incubated at 37  $^{\circ}\text{C}$  overnight. The  $\text{OD}_{600}$  value in each well was recorded to determine the bacterial growth. The  $\text{OD}_{600}$  value of the broth was used as a reference to determine the complete

inhibition of bacterial growth, and the  $\text{OD}_{600}$  value of the bacterial solution without any reagent was used as a positive control.

### Supplementary data

Spectroscopic information for the synthesized compounds and data for MIC determination are presented.

**Acknowledgements** This work was supported by the University of the Pacific. We also thank Dr. William K. Chan for providing MCF-7 and HeLa cells.

### Compliance with ethical standards

**Conflict of interest** The authors declare that they have no conflict of interest.

### References

- Ambrus A, Chen D, Dai J, Bialis T, Jones RA, Yang D (2006) Human telomeric sequence forms a hybrid-type intramolecular g-quadruplex structure with mixed parallel/antiparallel strands in potassium solution. *Nucleic Acids Res* 34:2723–2735
- Arya DP, Micovic L, Charles I, Coffee Jr. RL, Willis B, Xue L (2003a) Neomycin binding to Watson-Hoogsteen (W-H) DNA triplex groove: a model. *J Am Chem Soc* 125:3733–3744
- Arya DP, Xue L, Tennant P (2003b) Combining the best in triplex recognition: synthesis and nucleic acid binding of a BQQ-neomycin conjugate. *J Am Chem Soc* 125:8070–8071
- Arya DP, Xue L, Willis B (2003c) Aminoglycoside (neomycin) preference is for a-form nucleic acids, not just RNA: results for a competition dialysis study. *J Am Chem Soc* 125:10148–10149
- Balouiri M, Sadiki M, Ibensouda SK (2016) Methods for in vitro evaluating antimicrobial activity: a review. *J Pharm Anal* 6:71–79
- Blount KF, Tor Y (2006) A tale of two targets: differential RNA selectivity of nucleobase-aminoglycoside conjugates. *ChemBioChem* 7:1612–1621
- Degtyareva NN, Gong C, Story S, Levinson NS, Oyeler AK, Green KD, Garneau-Tsodikova S, Arya DP (2017) Antimicrobial activity, AME resistance, and A-site binding studies of anthraquinone-neomycin conjugates. *ACS Infect Dis* 3:206–215
- Edward Lindsell W, Murray C, Preston PN, Woodman TAJ (2000) Synthesis of 1,3-diynes in the purine, pyrimidine, 1,3,5-triazine and acridine series. *Tetrahedron* 56:1233–1245
- Fourmy D, Recht MI, Puglisi JD (1998) Binding of neomycin-class aminoglycoside antibiotics to the a-site of 16 s rRNA. *J Mol Biol* 277:347–362
- Fridman M, Belakhov V, Yaron S, Baasov T (2003) A new class of branched aminoglycosides: pseudo-pentasaccharide derivatives of neomycin b. *Org Lett* 5:3575–3578
- Grau-Campistany A, Massaguer A, Carrion-Salip D, Barragan F, Artigas G, Lopez-Senin P, Moreno V, Marchan V (2013) Conjugation of a ru(ii) arene complex to neomycin or to guanidino-neomycin leads to compounds with differential cytotoxicities and accumulation between cancer and normal cells. *Mol Pharm* 10:1964–1976
- Green KD, Chen W, Houghton JL, Fridman M, Garneau-Tsodikova S (2010) Exploring the substrate promiscuity of drug-modifying enzymes for the chemoenzymatic generation of n-acylated aminoglycosides. *ChemBioChem* 11:119–126

- Guckian KM, Schweitzer BA, Ren RX, Sheils CJ, Tahmassebi DC, Kool ET (2000) Factors contributing to aromatic stacking in water: evaluation in the context of DNA. *J Am Chem Soc* 122:2213–2222
- Guthrie OW (2008) Aminoglycoside induced ototoxicity. *Toxicology* 249:91–96
- Houghton JL, Green KD, Chen W, Garneau-Tsodikova S (2010) The future of aminoglycosides: the end or renaissance? *ChemBioChem* 11:880–902
- Kirk SR, Luedtke NW, Tor Y (2000) Neomycin–acridine conjugate: a potent inhibitor of rev-rre binding. *J Am Chem Soc* 122:980–981
- Liu M, Haddad J, Azucena E, Kotra LP, Kirzhner M, Mobashery S (2000) Tethered bisubstrate derivatives as probes for mechanism and as inhibitors of aminoglycoside 3'-phosphotransferases. *J Org Chem* 65:7422–7431
- Liu W, Minier MA, Franz AH, Curtis M, Xue L (2011) Synthesis of nucleobase-calix[4]arenes via click chemistry and evaluation of their complexation with alkali metal ions and molecular assembly. *Supramol Chem* 23:806–818
- Liu W, Wang S, Dotsenko IA, Samoshin VV, Xue L (2017) Aryl-sulfanyl groups-suitable side chains for 5-substituted 1,10-phenanthroline and nickel complexes as g4 ligands and telomerase inhibitors. *J Inorg Biochem* 173:12–20
- Lu W, Sengupta S, Petersen JL, Akhmedov NG, Shi X (2007) Mitsunobu coupling of nucleobases and alcohols: An efficient, practical synthesis for novel nonsugar carbon nucleosides. *J Org Chem* 72:5012–5015
- Oliveira JF, Silva CA, Barbieri CD, Oliveira GM, Zanetta DM, Burdmann EA (2009) Prevalence and risk factors for aminoglycoside nephrotoxicity in intensive care units. *Antimicrob Agents Chemother* 53:2887–2891
- Ramirez MS, Tolmasky ME (2010) Aminoglycoside modifying enzymes. *Drug Resist Updat* 13:151–171
- Vakulenko SB, Mobashery S (2003) Versatility of aminoglycosides and prospects for their future. *Clin Microbiol Rev* 16:430–450
- Wellenzohn B, Flader W, Winger RH, Hallbrucker A, Mayer E, Liedl KR (2001) Exocyclic groups in the minor groove influence the backbone conformation of DNA. *Nucleic Acids Res* 29:5036–5043
- Wong C-H, Hendrix M, Scott Priestley E, Greenberg WA (1998) Specificity of aminoglycoside antibiotics for the A-site of the decoding region of ribosomal RNA. *Chem Biol* 5:397–406
- Xue L, Charles I, Arya DP (2002) Pyrene–neomycin conjugate: dual recognition of a DNA triple helix. *Chem Commun* 70–71
- Xue L, Ling M, Wang S (2017) A reliable method to measure the melting temperatures of DNA oligonucleotide triplexes. *J Undergrad Chem Res* 16:19–23
- Xue L, Ranjan N, Arya DP (2011) Synthesis and spectroscopic studies of the aminoglycoside (neomycin)–perylene conjugate binding to human telomeric DNA. *Biochemistry* 50:2838–2849
- Zhang J, Keller K, Takemoto JY, Bensaci M, Litke A, Czyryca PG, Chang CW (2009) Synthesis and combinational antibacterial study of 5''-modified neomycin. *J Antibiot* 62:539–544